VERIZONA PUBLISHER
Publishing Your Ideas

www.verizonaonlinepublishing.com
Vol: 1, Issue: 3

Journal of Nanoscience with Advanced Technology

One-step Synthesis of Cetyltrimethylammonium Bromide Stabilized Spherical Gold Nanoparticles

Waqqar Ahmed[1,2], Jan M. van Ruitenbeek[1*]

[1]Huygens-Kamerlingh Onnes Laboratory, Niels Bohrweg 2, Leiden University, 2333 CA Leiden, The Netherlands

[2]Materials Laboratory, Department of Physics, COMSATS Institute of Information Technology, Islamabad, 44000, Pakistan

***Corresponding author:** Jan M. van Ruitenbeek, Huygens-Kamerlingh Onnes Laboratory, Niels Bohrweg 2, Leiden University, 2333 CA Leiden, The Netherlands; Tel: +31715275450; Fax: +31715275404; E mail: Ruitenbeek@physics.leidenuniv.nl

Article Type: Research, **Submission Date**: 9 November 2015, **Accepted Date:** 9 December 2015, **Published Date:** 8 January 2016.

Citation: Waqqar Ahmed and Jan M. van Ruitenbeek (2016) One-step Synthesis of Cetyltrimethylammonium Bromide Stabilized Spherical Gold Nanoparticles. J Nanosci Adv Tech 1(3): 20-24. doi: https://doi.org/10.24218/jnat.2016.13.

Abstract

For the synthesis of spherical Au nanoparticles (NPs), Turkevich method is very popular. However, in this method the citrate reduction of gold is carried out at high temperature, which is often a draw back. Herein, we describe a near room-temperature synthesis of cetyltrimethylammonium bromide (CTAB) stabilized spherical Au NPs of various sizes in a novel one-step synthesis protocol. We show that, in a growth solution containing CTAB, $HAuCl_4$ and ascorbic acid, nucleation can be induced by the addition of $AgNO_3$. This allowed us to eliminate the necessity of the presence of seed particles for NP growth. We show that NP size is strongly influenced by the CTAB to Ag molar ratio in the reaction medium. By tuning the CTAB to Ag molar ratio the sizes of the NPs can be tuned from 8 to 64 nm. Owing to the ease of synthesis and superior properties, CTAB stabilized NPs can replace the conventional citrate capped NPs for many applications.

Introduction

The shape and size dependent optical properties of Au NPs make them attractive for applications in photonics, sensing , catalysis and biomedicine [1-7]. There has been intense interest in developing protocols for size and morphology controlled synthesis of NPs. Among various synthesis methods, wet-chemical synthesis of Au NPs is simple, efficient and inexpensive. For the optimization of growth conditions and replication of recipes for more complex particle shapes, understanding the mechanism of growth in the wet-chemical synthesis is of crucial importance. However, the studies of the mechanisms involved are complicated by the presence of numerous reactants, as they often work in cooperation or in competition with one another. Therefore, well-established growth mechanisms are frequently challenged by new experimental findings.

For the synthesis of spherical Au NPs the Turkevich method is widely used. The method was initially developed by Turkevich et al. in 1951 and was later modified by many others [8-11]. In this method, anionic sodium citrate acts both as reducing and capping agent. This synthesis protocol has its advantages but the yield of low NP concentrations and need of high reaction temperatures (80-90°C) makes it inefficient especially for large scale production of NPs. More recently, a cationic surfactant CTAB has been used for the synthesis of Au NPs. The CTAB stabilized Au NPs are superior than their citrate capped counterparts for various applications [12-15]. For instance, the inter-particle repulsive interaction owing to the positively charged bilayer of CTAB on particle surface prevents random disordered aggregation of NPs during solvent evaporation [12]. Therefore, uniform inter-particle spacing equal to the length of CTAB molecule (2 nm) can be achieved on substrates making CTAB coated Au NPs excellent candidate for surface enhanced Raman spectroscopy [12]. The CTAB stabilized Au NPs also show excellent stability even under large salt concentration and low pH, whereas citrate capped Au NPs tend to agglomerate [15]. Furthermore, the synthesis of CTAB coated Au NPs can be carried out near room temperature which makes them economically viable for large scale production. However, for the synthesis of CTAB capped NPs in the size range of tens of nanometer, usually a seed-mediated, two-step method is followed [16-22]. First, seed particles are synthesized by reducing Au ions with a strong reducing agent, which are then added to a growth solution. The growth solution contains Au precursor, growth directional agents $AgNO_3$ and CTAB, and a weak reducing agent, ascorbic acid (AA). It is widely believed that AA can only reduce Au(III) to Au(I) in a low pH reaction medium [21,22]. Therefore, for complete reduction of Au ions, seed particles must be added to the growth solution [16,17]. The seed particles provide catalytic effect for the reduction of Au(I). Therefore, Au(I) ions are reduced on top of seed particles where they afterwards deposit.

We have recently reported the synthesis of worm-shaped Au NPs using a single-step, in which we have also observed that AA can completely reduce Au ions under high pH reaction conditions [23]. In this paper we report on the synthesis of spherical NPs of different sizes by a *seedless one-step reaction*. CTAB coated Au NPs

in the size range of 8-64 nm were synthesized by reducing Au ions with AA, under low pH conditions. Interestingly, the nucleation is induced by the addition of $AgNO_3$ in growth solution. We observe that the size of the NPs is strongly influenced by the ratio of CTAB to Ag ions in the reaction medium. We believe that the AgBr NPs that are possibly formed upon the addition of $AgNO_3$ in the reaction medium play the role of seeds facilitating the formation of larger Au NPs.

Experimental Methods

All chemicals were purchased from Sigma-Aldrich and were used as received without any further purification. For the preparation of solutions, Millipore water (18.2 MΩcm), was used.

For the synthesis of NPs, $HAuCl_4$ was added in 10ml of CTAB solution. The color of the solution at this stage was yellow. Next, a freshly prepared AA solution was added, which makes the solution colorless, indicating the reduction of Au ions. Finally, an $AgNO_3$ solution was added. The addition of $AgNO_3$ resulted in appearance of a brownish color, indicating the nucleation and growth of Au NPs. The solution was left undisturbed overnight at 25°C. Before imaging, the NP solution was centrifuged twice at 12000 rpm to remove excess CTAB, and redispersed in Millipore water.

Results and Discussion

Figure 1 depicts the spherical Au NPs prepared by various concentrations of CTAB while keeping the concentrations of the other reactants constant. Figure 1a shows a scanning electron microscopy (SEM) image of NPs prepared with the highest concentration of CTAB in solution (0.2M). The synthesized NPs are approximately spherical, having an average size of 39 nm. Reducing the CTAB concentration to 0.15M leads to a reduction of average particle size to 35 nm, as illustrated by Figure 1b. Further reduction in CTAB concentration reduces the particles size even further. Figure 1f depicts the variation of particle size with CTAB concentration. It is evident that the particle size decreases with decreasing CTAB concentration. Regardless of the CTAB concentration in the solution, only compact, nearly spherical NPs were obtained.

The NP size is also seen to be affected by the concentration of Ag ions in the solution, when CTAB concentration is kept constant. Figure 2(a-c) depicts Au NPs synthesized with a CTAB concentration of 0.05M, and $AgNO_3$ concentrations of 0.05mM, 0.10 mM and 0.6 mM, respectively. As is evident from the SEM images, the particle size decreases with increasing $AgNO_3$ concentration. Similarly, for 0.1M CTAB, the particle size decreases from 64 nm for 0.05mM $AgNO_3$ (Figure 2d) to 20 nm for 0.6 mM $AgNO_3$ (Figure 2e). As evident from Figure 2(f), for each $AgNO_3$ concentration, the particle size is larger for the CTAB concentration of 0.1 M in the solution as compared to 0.05 M. Note that in both cases (Figure 1 & Figure 2), particle size decreases with decreasing CTAB to Ag ratio.

Figure 3 shows the variation of particle size with CTAB to Ag ratio. The ratio is changed by independently varying the concentration of either CTAB or Ag, while keeping the concentration of the other one constant. The plot depicts that, although not perfect, the particle size has nearly liner dependence on CTAB to Ag molar ratio. These results clearly show that CTAB to Ag ratio plays a crucial role in controlling the particle size.

It is important to note that in the conventional methods of synthesis Ag ions are added in the reaction medium before the reduction of Au ions is initiated by AA. In contrast, in the method employed here Ag ions are added only after the reduction of Au ions by AA. Similar observations have been reported by Sau et al. during the synthesis of multi-spiked Au NPs [24]. They propose that Ag ions are first reduced, forming Ag(0) nuclei which lead to Au NP growth either by sacrificial oxidation of Ag or by Ag(0) nuclei serving as seeds and facilitating Au^+ reduction on their surface by a catalytic effect. On the other hand, many researchers have argued that AA cannot reduce Ag(I) (when it exists as AgBr in CTAB solution prior to adding AA), in an acidic reaction medium [25-28] like the one used for the current study. However, the monoanion of AA, ascorbate, is a stronger reducing agent than the AA itself [22, 29], and at high solution pH, it is able to undertake the reduction of Ag(I) in CTAB solution [18]. As the first pKa of AA is 4.1, only a small fraction of AA dissociates into ascorbate monoanions below the pH of 4.1 [22]. Consequently,

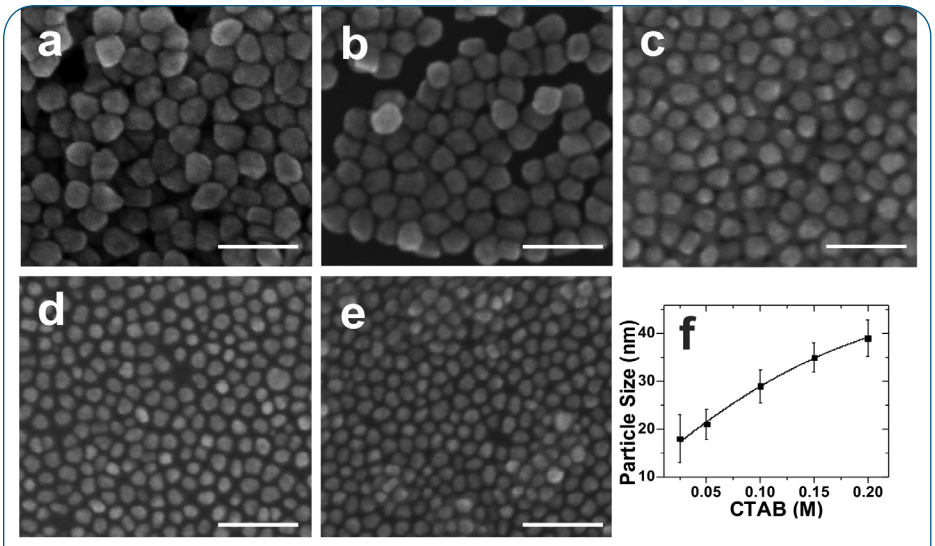

Figure 1: SEM image of Au NPs synthesized using $HAuCl_4$, AA and $AgNO_3$ concentrations of 1 mM, 1.1 mM and 0.2 mM, respectively. The CTAB concentration is 0.2M (a), 0.15M (b), 0.1M (c), 0.05M (d) and 0.025M (e). Variation of particle size with CTAB concentration is shown by (f). The scale bar is 100 nm

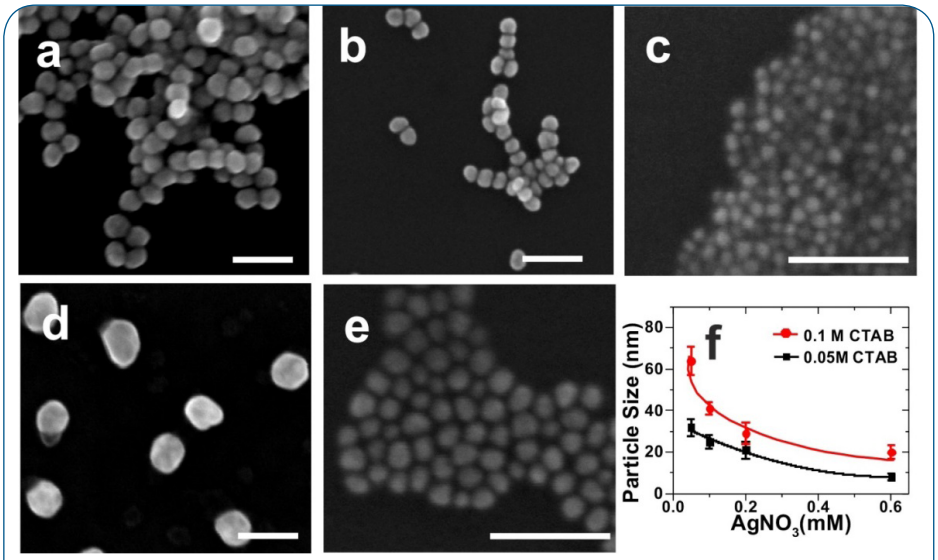

Figure 2: SEM image of Au NPs synthesized using $HAuCl_4$, and AA concentrations of 1 mM and 1.1 mM, respectively. The CTAB concentration is 0.05M (a-c) and 0.1 M (d, e); the $AgNO_3$ concentration is 0.05 mM (a), 0.1 mM (b), 0.6 mM(c), 0.05 mM(d) and 0.6 mM (e). The variation of particle size as a function of the $AgNO_3$ concentration is shown in panel (f). The curves serve as a guide to the eye. The scale bar in (a-e) is 100 nm, but please note the different length of this scale bar for (c) and (e)

reduction of preexisting Ag(I) by AA is difficult in acidic reaction conditions and in the presence of CTAB. Numerous studies have shown that Ag ions under such reaction conditions can only reduce to Ag(0) through the under potential deposition (UPD) on Au NP surfaces [20,30,31]. Consequently, Au ions have to be reduced first to metallic Au for the reduction of Ag ions to Ag(0).

However, one can assume that Ag is seen by AA as AgBr when the Ag salt is added before AA, while it encounters preexisting AA in solution as Ag^+ when it is added after AA. The reduction potentials of Ag(I) when it exists as Ag^+ and AgBr are +0.799V and +0.071V, respectively. Therefore, the reduction of Ag(I) is easier when it exits as Ag^+ compared to the case when it exists as AgBr. Consequently, the reduction of Ag(I) may be easier due to the presence of pre-existing AA in solution. If that happens, the switching of the addition of $AgNO_3$ and AA may lead to nucleation of Ag NPs. For higher concentrations of $AgNO_3$, higher number of Ag NP seeds may form. The same amount of Au ions in reaction medium, and greater number of Ag seeds would lead to a smaller final Au NP size. This might explain the decrease in particle size with increasing $AgNO_3$ concentration in reaction medium. However, increase in particle size with increasing CTAB concentration, for the same amount of $AgNO_3$, cannot be explained by the argument of Ag NPs formation.

Another possibility of initiation of growth of Au NPs with the addition of Ag ions in reaction medium is due to the formation of AgBr NPs. AgBr NPs can form when Ag is added in a medium containing CTAB. The yield of AgBr NPs is very sensitive to the chemical environment [32, 33]. This could be the reason that AgBr NPs are only formed when $AgNO_3$ is added after the addition of AA, and not the other way around.

Chakraborty et al showed that AgBr NPs can be obtained by progressive addition of $AgNO_3$ in CTAB solution [32]. AgBr NPs are semiconductors with an indirect bandgap of 2.3eV (absorption edge at 477nm). Therefore, electrons can be excited to the conduction band by visible light. These optically excited electrons, present in the conduction band of AgBr NP, can act as a reducing agent to catalyze the reduction of metal ions [34]. Therefore, AgBr NPs can play the role of seeds for the growth of Au NPs by a catalytic effect for reduction of Au(I) to Au(0).

The increase in particle size with increasing CTAB to Ag molar ratio can also be explained if one assumes that AgBr seeds cause Au NP formation. Chakraborty et al postulated that for higher concentrations of CTAB in solution larger numbers of micelles are formed [32]. For the same concentration of Ag ions and more CTAB micelles, the average number of Ag ions per CTAB micelle decreases and hence the probability of achieving critical number of AgBr monomers for the nucleation of AgBr within a micelle decreases. Therefore, higher CTAB concentrations lead to lower number of AgBr NPs. On the other hand, a higher Ag ion concentration in solution, for same amount of CTAB, would imply a larger number of Ag ions per CTAB micelle. Hence the probability of AgBr nuclei formation increases. Therefore, larger numbers of AgBr NPs are formed for higher Ag ion concentration in solution. Consequently, the number of AgBr nuclei is lower for higher CTAB to Ag molar ratios [32]. For the same amount of Au ions in solution, less AgBr seeds lead to the formation of larger NPs. This explains the increase in size of NPs by increasing the CTAB concentration in solution (Figure 1). Similarly, the decrease in particle size with increasing $AgNO_3$ concentration (Figure 2) can also be understood by the reasoning presented here. In both cases, the CTAB to Ag ratio changes leading to a change in particle size.

Another important ratio for controlling the reaction kinetics is the AA to Au ratio. It is know that each molecule of AA can only donate two electrons. Therefore, for complete reduction of all Au ions, one would need at least a AA to Au ratio of 1.5 [17]. Here we are using an AA to Au ratio of 1.1. Therefore, only a fraction of Au ions are completely reduced to Au(0) and hence we expect a limited supply of monomers for growth of

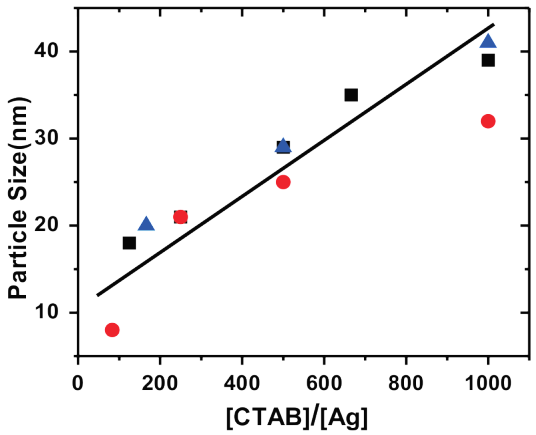

Figure 3: Variation of particle size with CTAB to Ag molar ratio. Black squares, red circles and blue triangles represent samples prepared with a fixed $AgNO_3$ concentration of 0.2 mM, fixed CTAB concentration of 0.05M and fixed CTAB concentration of 0.1 M, respectively. The curve serves as guide to the eye

NPs. Under such reaction conditions the growth rate of all the facets seems to be the same as a spherical morphology results (Figure 1, 2). The growth kinetics can be changed by having a higher concentration of AA in solution. A higher concentration of AA would lead to faster growth kinetics leading to different particle morphology. Figure 4(a,b) depicts the particles prepared by using AA to Au molar ratio of 1.5 and 10, respectively. The resultant particle shapes deviate from the spherical shapes seen in Figures 1 and 2. We observe a range of different particle shapes such as octahedra, truncated ditetragonal and trisoctahedra. The polydispersity in shape is indicative of poorly controlled growth probably due to a fast growth rate. Nonetheless, an important conclusion that can be drawn from this is that at higher AA to Au ratios, the growth rate of different facets is not the same. We believe that slight tuning of the reaction conditions may lead to yield of highly monodispersed NPs of various shapes. Further work on the synthesis of different particle shapes by our one-step method is under way.

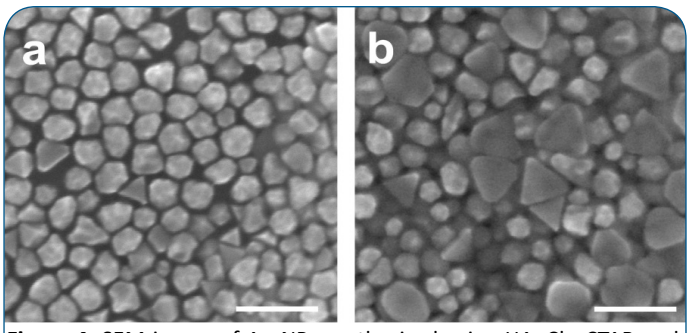

Figure 4: SEM image of Au NPs synthesized using $HAuCl_4$, CTAB and $AgNO_3$ concentrations of 1 mM, 0.1 M and 0.2 mM, respectively. The AA concentration is 1.5 mM (a), and 10 mM (b). The white scale bar is 100nm

Conclusion

In conclusion, we demonstrated that Au NPs can be synthesized by a single step near room temperature. We show that, contrary to the widely accepted views, nucleation and growth of Au NP can be achieved by reducing Au ions with AA, without the need of addition of separately prepared seeds or a stronger reducing agent in the reaction medium. Consequently, two step synthesis protocol can be reduced to a single step for the synthesis of spherical NPs in a wide size range. We have seen that the size of the NPs is strongly influenced by Ag to CTAB molar ratio in the reaction medium. The NP size can be controlled by tuning the Ag to CTAB ratio. Finally, particle shapes can be tuned by using higher concentrations of the reducing agent AA.

Acknowledgment

This work is part of the Industrial Partnership Programme (IPP) Innovative Physics for Oil and Gas (iPOG) of the Stichting voor Fundamenteel Onderzoek der Materie (FOM), which is supported financially by Nederlandse Organisatie voor Wetenschappelijk Onderzoek (NWO). The IPP iPOG is co-financed by Shell.

References

1. Daniel MC, Astruc D. Gold nanoparticles: assembly, supramolecular chemistry, quantum-size-related properties, and applications toward biology, catalysis, and nanotechnology. Chem Rev. 2003; 104(1):293–346.
2. Sardar R, Funston AM, Mulvaney P, Murray RW. Gold nanoparticles: past, present, and future. Langmuir. 2009; 25(24):13840–13851. doi: 10.1021/la9019475.
3. Ray PC. Size and shape dependent second order nonlinear optical properties of nanomaterials and their application in biological and chemical sensing. Chem Rev. 2010; 110(9):5332−5365. doi: 10.1021/cr900335q.
4. Han J, Liu Y, Guo R. Facile synthesis of highly stable gold nanoparticles and their unexpected excellent catalytic activity for Suzuki−Miyaura cross-coupling reaction in water. J Am Chem Soc. 2009; 131(6):2060−2061. doi: 10.1021/ja808935n.
5. Fasciani C, Alejo CJB, Grenier M, Netto-Ferreira JC, Scaiano JC. High-temperature organic reactions at room temperature using plasmon excitation: decomposition of dicumyl peroxide. Org Lett. 2011; 13(2):204−207. doi: 10.1021/ol1026427.
6. He H, Xie C, Ren J. Nonbleaching fluorescence of gold nanoparticles and its applications in cancer cell imaging. Anal Chem. 2008; 80(15):5951−5957. doi: 10.1021/ac8005796.
7. Niidome T, Nakashima K, Takahashi H, Niidome Y. Preparation of primary amine-modified gold nanoparticles and their transfection ability into cultivated cells. Chem Commun (Camb). 2004; 17:1978−1979.
8. Turkevich J, Stevenson PC, Hillier JA. Study of the nucleation and growth processes in the synthesis of colloidal gold. Disc Faraday Soc. 1951; 11:55-75. doi: 10.1039/DF9511100055.
9. Frens G. Controlled nucleation for regulation of particle-size in monodisperse gold suspensions. Nat. Phy. Sci. 1973; 241:20-22. doi:10.1038/physci241020a0.
10. Chow MK, Zukoski CF. Gold sol formation mechanisms-role of colloidal stability. J Coll Inter Sci. 1994; 165(1):97-109. doi:10.1006/jcis.1994.1210.
11. Li C, Li D, Wan G, Xu J, Hou W. Facile synthesis of concentrated gold nanoparticles with low size-distribution in water: temperature and pH controls. Nanoscale Res Lett. 2011; 6(1):440. doi: 10.1186/1556-276X-6-440.
12. Wang H, Levin CS, Halas NJ. Nanosphere arrays with controlled sub-10-nm gaps as surface-enhanced Raman spectroscopy substrates. J Am Chem Soc. 2005; 127(43):14992-14993.

13. Narayanan R, Lipert RJ, Porter MD. Cetyltrimethylammonium bromide-modified spherical and cube-like gold nanoparticles as extrinsic Raman labels in surface-enhanced Raman spectroscopy based heterogeneous immunoassays. Anal Chem. 2008; 80(6):2265–2271. doi: 10.1021/ac7026436.

14. Fenger R, Fertitta E, Kirmse H, Thünemannc AF, Rademann K. Size dependent catalysis with CTAB-stabilized gold nanoparticles. Phys Chem Chem Phys. 2012; 14(26):9343-9349. doi: 10.1039/c2cp40792b.

15. Baruah B, Craighead C, Abolarin C. One-phase synthesis of surface modified gold nanoparticles and generation of SERS substrate by seed growth. Langmuir. 2012; 28(43):15168–15176. doi: 10.1021/la302861b.

16. Murphy CJ, Jana NR. Controlling the aspect ratio of inorganic nanorods and nanowires. Adv. Mater. 2002; 14(1):80-82. doi: 10.1002/1521-4095(20020104)14:1<80::AID-ADMA80>3.0.CO;2-#.

17. Nikoobakht B, El-Sayed MA. Preparation and growth mechanism of gold nanorods (NRs) using seed-mediated growth method. Chem Mater. 2003; 15(10):1957-1962. doi: 10.1021/cm020732l.

18. Jana NR, Gearheart L, Murphy CJ. Seed-mediated growth approach for shape-controlled synthesis of spheroidal and rod-like gold nanoparticles using a surfactant template. Adv. Mater. 2001; 13(18):1389-1393. doi: 10.1002/1521-4095(200109)13:18<1389::AID-ADMA1389>3.0.CO;2-F.

19. Hubert F, Testard F, Spalla O. Cetyltrimethylammonium bromide silver bromide complex as the capping agent of gold nanorods. Langmuir. 2008; 24(17):9219-9222. doi: 10.1021/la801711q.

20. Liu M, Guyot-Sionnest P. Mechanism of silver (I)-assisted growth of gold nanorods and bipyramids. J Phys Chem B. 2005; 109(47):22192–22200.

21. Ahmed W, Kooij ES, van Silfhout A, Poelsema B. Controlling the morphology of multi-branched gold nanoparticles. Nanotechnology. 2010; 21(12):125605. doi: 10.1088/0957-4484/21/12/125605.

22. Busbee BD, Obare SO, Murphy CJ. An improved synthesis of high-aspect-ratio gold nanorods. Adv Mater. 2003; 15(5):414-416. doi: 10.1002/adma.200390095.

23. Ahmed W, Glass C, van Ruitenbeek JM. Facile synthesis of gold nanoworms with a tunable length and aspect ratio through oriented attachment of nanoparticles. Nanoscale. 2014; 6:13222-13227. doi: 10.1039/C4NR04122D.

24. Sau TK, Rogach AL, Döblinger M, Feldmann J. One-step high-yield aqueous synthesis of size-tunable multispiked gold nanoparticles. Small. 2011; 7(15):2188-2194. doi: 10.1002/smll.201100365.

25. Chen SH, Carroll DL. Silver nanoplates: size control in two dimensions and formation mechanisms. J. Phys. Chem. B. 2004; 108(18):5500-5506. doi: 10.1021/jp031077n.

26. Jana NR, Gearheart L, Murphy CJ. Wet chemical synthesis of silver nanorods and nanowires of controllable aspect ratio. Chem Commun. 2001:617-618. doi: 10.1039/B100521I.

27. Lu L, Kobayashi A, Tawa K, Ozaki Y. Silver nanoplates with special shapes: controlled synthesis and their surface plasmon resonance and surface-enhanced Raman scattering properties. Chem Mater. 2006; 18(20):4894-4901. doi: 10.1021/cm0615875.

28. Grzelczak M, Pérez-Juste J, Mulvaney P, Liz-Marzán LM. Shape control in gold nanoparticlesynthesis. Chem Soc Rev. 2008**;** 37:1783-1791. doi: 10.1039/B711490G.

29. Pal T, Jana NR, Pradhan N, Mandal R, Pal A, Beezer AE, et al. Organized media as redox catalysts. Langmuir. 1998; 14(17):4724-4730. doi: 10.1021/la980057n.

30. Seo D, Park JC, Song H. Polyhedral gold nanocrystals with Oh symmetry: from octahedra to cubes. J Am Chem Soc. 2006; 128(46):14863–14870.

31. Zhang J, Langille MR, Personick ML, Zhang K, Li S, Mirkin CA. Concave cubic gold nanocrystals with high-index facets. J. Am. Chem. Soc. 2010; 132(40):14012–14014. doi: 10.1021/ja106394k.

32. Chakraborty M, Hsiao FW, Naskar B, Chang CH, Panda AK. Surfactant-assisted synthesis and characterization of stable silver bromide nanoparticles in aqueous media. Langmuir. 2012; 28(18):7282–7290. doi: 10.1021/la300615b.

33. Husein MM, Rodil E, Vera JH. Preparation of AgBr nanoparticles in microemulsions via reaction of AgNO3 with CTAB Counterion. J. Nanopart. Res. 2007; 9(5):787-796. doi: 10.1007/s11051-006-9107-4.

34. Zhang H, Cao L, Liu W, Su G, Gaob R, Zhao Y. The key role of nanoparticle seeds during site selective growth of silver to fabricate core–shell or asymmetric dumbbell heterostructures. Dalton Trans. 2014; 43:4822–4829. doi: 10.1039/C3DT53207K.